Impact of nanodrops on smooth surfaces with various wettabilities: splash phenomena and film dewetting

Bertrand Braeckeveldt[1], Juan Carlos Fernandez-Toledano [1], Marco Marengo[2], Joël De Coninck[*1]
[1]Laboratory of Physics of Surfaces and Interfaces, Department of Physics, University of Mons, Mons, Belgium
[2]School of Computing, Engineering and Mathematics, University of Brighton, Brighton BN2 4GJ, U.K.
*Corresponding author: Joel.DECONINCK@umons.ac.be

Abstract
Interaction of nanodroplet with surfaces is a fascinating novel subject with potential major impact for nanomedicine, 3D nanoprinting, nanoscale liquid impingement, phase-change cooling using nanosprays and for special material microdeposition processes. The impact of nanometer sized drops on smooth solid surfaces is studied using molecular dynamics simulations. Using LAMMPS software, we study in details the impact of slice of drops on substrates. This allows to consider in a reasonable amount of time systems which can reach significantly larger sizes along the x-z directions. We have first validated this approach by studying the dynamics of spontaneous wetting for the corresponding sliced droplet. We prove that this technique allows to recover exactly previous results obtained for truly three dimensional nanodroplets in the same conditions. We then generalize this study by considering an impact speed. Nanodrops impacting at low velocity bounce from non-wetting surfaces but stick and subsequently spread on wetting surfaces. Higher velocity impacts onto a wetted surface produce a crown splash like it is usually observed for larger drops. Impact velocity, liquid-solid coupling and film thickness are the parameters which affect dewetting. Increasing the velocity of the droplet will help to dewet while increasing the coupling will lead to more resistant film. Results showed that the dewetting speed depends on the thickness of the film and the coupling. Even if the drop spreading can be analysed in terms of Weber and Reynolds as for millimetric droplets, a modification of the standard map of the impact regimes is necessary to take into account the adhesion forces between the liquid and the atomic solid surface. Our results show the ability of molecular dynamics to provide a detailed look on how impact can induce a splash and a dewetting phenomenon. This may help the design of nanoprinters, since it is giving an estimation of the maximum impact velocities in order to obtain a smooth and homogenous coverage of the surfaces without dry spots. Results are also encouraging and stimulating to use these techniques to study heat transfer at the nanoscale during dewetting.

Keywords
Droplet impact, molecular dynamics, wettability, nanoscale

Introduction

In this study we focus on the impact of nanodroplets (typically the radius equals $17\mathrm{nm}$) on flat solid substrates. To handle this problem we use molecular dynamics. Because this method is not based on meshes but compute directly the forces acting between atoms via the Newton's law, we does not need to make any hypothetical supposition on boundary conditions. Furthermore we have a direct access to flows during the process and so we have a molecular resolution on the whole mechanism. MD allows us to tune fundamental parameters like strength of interactions between atoms in order to explore the details of this phenomenon. Finally there are more and more real live applications which demand better understanding of this process. We can cite nanomedicine, 3D nanoprinting, nanoscale liquid impingement, phase-change cooling using nanosprays and microdeposition processes.
In this study, we work with a slice of drop (or cylindrical drop) because it allows either to consider bigger system in x and z directions or to reduce the computation time. First we show that with such a system we can recover results obtained with a full 3D system validating in that way our approach. In the second part we consider drop impacts on solid substrates. Then we study the effect of the impact velocity trough the Weber number and finally the effect of the substrate wettability is considered by tuning the amplitude of the interaction between the liquid and the solid.

Numerical modelling set-up

The tool used to realise all the simulations presented herewith is LAMMPS [1]. The considered liquid is a simple Lennard-Jones model which has been already widely studied in previous paper [2, 3, 4]. It has been shown that with this model we can recover important results as the Young's law governing liquid/vapor/solid interfaces.
The liquid is made of 8-atoms molecules in order to increase the viscosity and to reduce evaporation. Atoms are linked through a FENE potential which can be written

$$V_{FENE} = -0.5 k_L R_0^2 \ln\left[1 - \left(\frac{r}{R_0}\right)^2\right], \tag{1}$$

This work is licensed under a Creative Commons 4.0 International License (CC BY-NC-ND 4.0).

and thus the maximum extension length between two adjacent atoms is R_0.
The solid substrate is simply modelled as a set of atoms which are allowed to vibrate around an equilibrium position. Each of these atoms is linked to a predefined position by an harmonic potential. Basically the model aims to represent the thermal vibrations. The corresponding potential is given by

$$V_{harm} = k_S \left(r - r_0\right)^2, \tag{2}$$

where r_0 represents the equilibrium position and k_S the stiffness of the link.
All the atoms interact between each other via a pairwise Lennard-Jones potential

$$V_{ij} = -4C_{AB}\ \varepsilon_{ij} \left[\left(\frac{\sigma_{ij}}{r_{ij}}\right)^6 - \left(\frac{\sigma_{ij}}{r_{ij}}\right)^{12} \right]. \tag{3}$$

Index of atoms are denoted with i and j and the "type" of atoms (liquid or solid) is denoted through the letter "A" or "B". The depth of the potential and the effective molecular diameter are respectively ε_{ij} and σ_{ij}. By tunning the value of C_{AB} (coupling between type "A" and type "B") we are able to change the strength of the interaction between the two types of atoms. Large coupling will lead to a strong interaction and a weak coupling will lead to a small interaction. In our simulations we choose to put the same diameter and same mass for all atoms that we decided to be carbon-like. Therefore σ is set to 3.5 Å and m, the mass of atoms to 12 $\mathrm{g/mol}$. Each simulation consists of two steps. In the first one, we equilibrate the system and thus keep the temperature constant. This is realized by rescaling all the velocities in order to reach a constant temperature of 33 K. Indeed the temperature is linked to the kinetic energy through the well known relation

$$\frac{1}{2} m \overline{v^2} = \frac{3}{2} k_B T. \tag{4}$$

The variable ε is set to $\mathcal{N}_A k_B T$ $\mathrm{kcal/mol}$ and K_L, K_S respectively to ε and 10ε $\mathrm{k/s^2}$. Finally R_0 is equal to 1.4σ.
If we do not set a cut off radius for the computation of interactions between atoms, the software will explore all pairs of atoms and thus it will increase the computation time. So, it has been shown that a cut-off of 2.5σ is a good compromise between computation time and accuracy.
Discrete timestep between each interaction evaluation was fixed to 5 fs. In molecular dynamics we have to define boundary conditions in the three directions of space. These conditions are periodic along x and y (direction parallel to the substrate) and non periodic along z (direction perpendicular to the substrate).
Before considering the impact of the nanodroplet on the substrate, the whole system must be at equilibrium. To begin, a rectangular set of molecules which will form the droplet is positioned far from the solid substrate as shown in Figure 1. Initially, we assign a random velocity to the atoms according to the Boltzmann distribution associated to the desired temperature (33 K). For each type of atoms an independent thermostat is used and the total energy is monitored. The equilibrium stage is achieved when the energy is constant versus time and the droplet shows a circular shape.
After the equilibration step, the thermostat of the liquid is removed in order to enable thermal exchanges between the two kind of atoms. The drop is also displaced a few angstroms above the substrate so as to reduce the distance to cross before impact. Finally, an initial velocity in the z direction (perpendicular to the solid) is set to the drop in order to initiate the impact.

To study nanodroplet impacts on substrate there are many variables that can be tuned to better understand the underlying mechanisms governing this process. Nevertheless it is not reasonable to change all the parameters in the same time so we decide to focus on some of them. We keep constant the size along the y direction (thickness of the droplet slice) and the droplet volume. The substrate is always a four atoms thick flat solid. We tune the coupling between liquid and solid atoms as well as the impact velocity. Changing the coupling enables us to explore different wettabilities and thus study in details the importance of this parameter at the nano-scale. The length of the plate (x direction) is changed depending on the droplet velocity. Indeed if the velocity is too high and the plate too short, the periodical boundary conditions can be a problem. But for small velocity reducing the length of the plate enables to decrease the computation time. The Table 1 gathers all the informations about the sizes of the studied systems and the number of atoms contained in the droplet.
The Table 2 gives some important properties of the liquid we used.

Table 1. Dimension of the simulation box and details on the droplet

Box dimension ($x \times y \times z$) (nm)	# droplet atoms	Droplet radius (nm)
(117.86 $\rightarrow$ 392.86) $\times$ 3.14 $\times$ 50.50	51 200	17.34 $\pm$ 0.66

.

This work is licensed under a Creative Commons 4.0 International License (CC BY-NC-ND 4.0).

Table 2. Property of the Lennard-Jones liquid

Surface tension ($\mathrm{mN/m}$)	Viscosity ($\mathrm{mPa\,s}$)	Density ($\mathrm{kg/m^3}$)
2.85 $\pm$ 0.56	0.248 $\pm$ 0.004	386$\pm$ 5

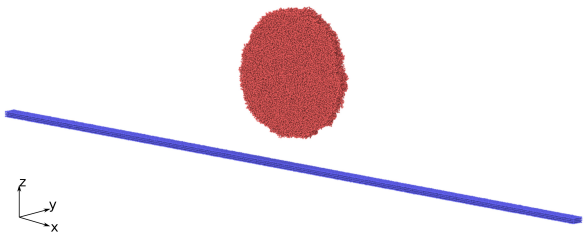

Figure 1. Configuration – Axes of the system

Spontaneous wetting case

Because we do not use a 3D spherical droplet, we first need to validate the model. The droplet is considered as a slice of drop with a given thickness so it is not totally a 2D system. The configuration of the system is shown in Figure 1. As shown in this picture, the thickness of the slice is considered along the y axis.

The spontaneous wetting has been studied in order to validate our quadi 2D model. Indeed, this problem has already been studied with the same approach (molecular dynamics simulation with a Lennard-Jones liquid) but in a fully 3 dimensional simulation [5]. We can therefore have an interesting point of comparison to validate the slice model. To achieve a spontaneous spreading in our simulation, we displace, after the equilibration of the system, the droplet just above the substrate so as to let liquid solid interactions initialize the spreading. Two different parameters are compared. First, we analyse the equilibrium contact angle. It depends on the coupling C_{LS} where "L" represents atoms of liquid and "S" atoms of solid. For the recording of the contact angle with time, an home-made python-script was used. It consists of the location of droplet edges via the variation of the liquid density ρ_L along the x axis. This variation can be expressed as

$$\rho_L = \frac{1}{2}\rho_0 \left[1 \pm \tanh\left(\frac{2(x - x_e)}{d}\right)\right] \tag{5}$$

where the "+" sign is used to fit the left part of the droplet and the "-" for the right part. When the liquid density reaches half of its maximum value, it marks the location of the liquid vacuum interface and thus a drop edge. Because the droplet must be circular during a spontaneous spreading, we decided to fit a circle from the computed edges. With this circle it is then simple to extract the contact angle for a given timestep if the location of the substrate is known.

In order to obtain an accurate value for the equilibrium contact angle, a systematic process is used on all the simulations. First, we measure the mean contact angle $\bar{\theta}$ on time windows represented by the region between two successive black lines in Figure 2. Then the mean contact angle $\bar{\theta}_n$ is computed from the nth time windows and is compared to the one from the window $n-1$. When $|\bar{\theta}_{n-1} - \bar{\theta}_n|$ is under a given tolerance ε_{tol}, the system can be considered as equilibrated. So finally, we compute the mean angle from this point to the end of the simulation to obtain the equilibrium angle θ_{eq}.

Because the choice of ε_{tol} can not be arbitrary, various values were tested. In our case consider ε_{tol} below 0.1° does not significantly change the evaluated equilibrium angle. Furthermore, choose a too small value for the tolerance can leads to an artificial reduction of the error. The red window in Figure 2 shows an example of the equilibrium region for a coupling C_{LS} of 0.8.

We computed the equilibrium angle for couplings from 0.2 to 1 and we compared those values to the one of the 3D system already studied in [5]. The effect of the coupling on droplet final state is shown in Figure 3. Angles comparison is presented in Figure 4. It shows that the equilibrium angles for our quasi 2D approach are very compatible with the full 3D simulation results. There is in fact a very small deviation for a few coupling values (like 0.8) but this is not a significant deviation .

Now, let us present the other validation test, the contact line friction computation. Because the angle changes with time during spreading, there must be an underlying dissipation process. It is why we are interested in the contact line friction. In oder to obtain this value, we have to use the molecular kinetic theory (MKT) [6] and in particular, the linear regime of this theory. In the linear MKT, the velocity of the contact line, so the velocity of the triple line is directly related to the driving force, here the capillary force, by the inverse of the contact line friction. Mathematicaly it can be expressed as,

$$V_{CL}(t) = \frac{\gamma_L}{\zeta^0_{CL}} \left(\cos\theta_{eq} - \cos\theta_D(t)\right). \tag{6}$$

where ζ^0_{CL} refers to the contact line friction and $\theta_D(t)$ the dynamic angle. The liquid surface tension is denoted by γ_L and its value can be found in Table 2. So in order to compute the contact line friction, we use linear fits of

This work is licensed under a Creative Commons 4.0 International License (CC BY-NC-ND 4.0).

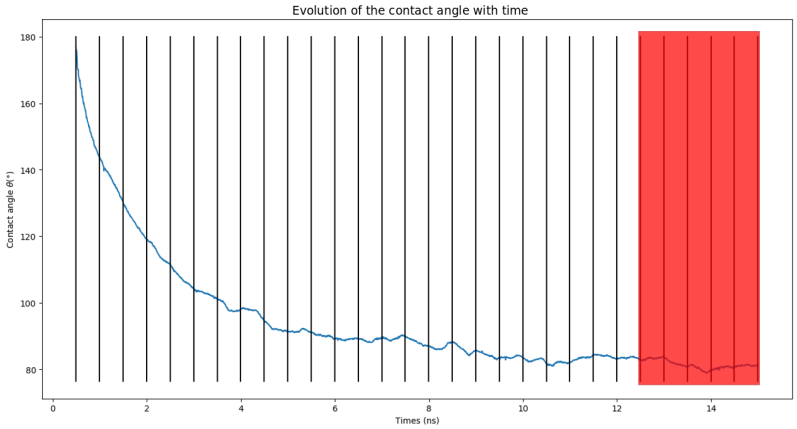

Figure 2. Variation of the contact angle with time – Computation of the equilibration angle

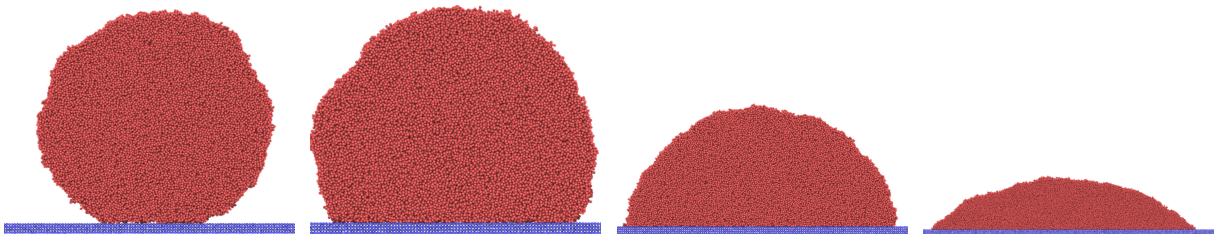

(a) C_{LS}=0.2 (b) C_{LS}=0.5 (c) C_{LS}=0.8 (d) C_{LS}=1

Figure 3. Effect of the liquid solid coupling C_{LS} on the spreading

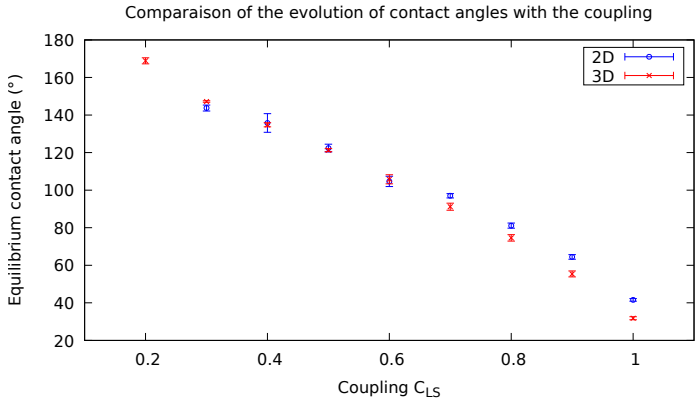

Figure 4. Equilibrium angle comparison. Slice model vs fully 3D model

the driving force versus the contact line velocity. The corresponding slopes corresponds thus to the ratio γ_L/ζ^0_{CL}. We have already presented the way we compute the dynamic angle but we also have to compute the contact line velocity. Thanks to the circular fit we used to obtain $\theta_D(t)$, we have also access to the contact radius with time $R(t)$. So we use a ratio of quadratic polynomial to obtain an analytical form of the evolution of this radius. This ratio is a five parameters expression,

$$R(t) = \frac{a_1(t-t_0) + a_2(t-t_0)^2}{1 + a_3(t-t_0) + a_4(t-t_0)^2} \tag{7}$$

where a_1 to a_4 and t_0 are the parameters. The value of t_0 give the starting point of the spreading process because it corresponds to $R = 0$. The derivative of the corresponding fitted function thus give the contact line velocity.
The linear regime typically appends when this velocity is below $4\mathrm{m/s}$. The comparison of ζ^0_{CL} obtained values with the three dimensional system is given in Figure 5. It shows that the differences between these two values are within error bars. It must also be said that, for the linear fit, the determination coefficient R^2 is computed. It is never below 0.9 showing that the regime was well linear. One more time we see that the quasi 2D model enables to recover the same dynamics as a fully 3D model. But, as we said earlier, a quasi 2D model will allow to study bigger system in x

This work is licensed under a Creative Commons 4.0 International License (CC BY-NC-ND 4.0).

direction and consider bigger droplet without computation time limitation. From now, presented result are obtained from the slice model because we showed that the spreading dynamics is the same as the 3D one.

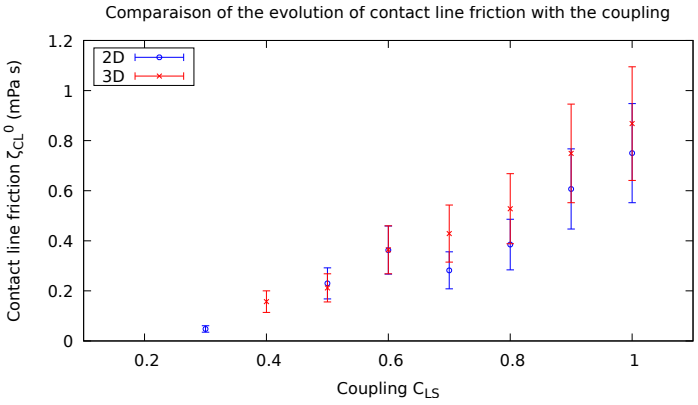

Figure 5. Contact line friction comparison. Slice model vs fully 3D model

MD simulations of nanodrop impacts

We are now interested in spreading with an impact speed. Thus the spreading is now no longer governed by the same laws and parameters as before. Many correlations and models have been proposed in literature [7, 8, 9, 10, 11], as well as 1D analytical models [12, 13, 14], which predict time evolution of spread factor

$$\xi(t) = \frac{D(t)}{D_0}. \tag{8}$$

These correlations are empirical or semi-empirical and were obtained mostly by curve fitting. In this sense they can not be accepted as general law. Moreover, none of these correlations correctly take into account the wettability effect. MD simulations appear to be a good way to study in details these effects. In order to compare our results, we have to use dimensionless numbers and in particular the Weber number,

$$We = \frac{\rho_L D_0 v^2}{\gamma_L} \tag{9}$$

which is the ratio of the liquid inertia and the surface tension. We have also to define some parameters used in drop impact study. The first one is the drop maximum spreading $\xi_{max} = D_{max}/D_0$, ratio between the maximum contact diameter and the drop initial diameter. The second one is the spreading time t_s which is the time when $\xi(t) = \xi_{max}$. And finally the time at maximum spreading $\Delta t_{\xi_{max}}$ which is the time delay between the moment drop stops spreading and the moment drop starts receding.

Spreading and max spreading

In the case of a "forced" spreading, the droplet does not keep a circular shape during the process. We thus have to change the way we compute the contact diameter. In this case, the droplet can be fitted with an ellipse. Edges can be obtained by the density variation if Weber number values are not too high. For high Weber values, edges are extracted via pictures created with OVITO from atom positions [15]. So a home made python script for droplet image edges detection is used after validation for the previously considered spontaneous case. .

In Figure 6 we show two typical examples of the spreading dynamics in the case of an impact. We can already see that the wettability affects the maximum spreading value. This value will be bigger if the substrate is more hydrophobic. This figure also shows that in the higher coupling case (so substrate less hydrophobic), the droplet needs more time to recover is equilibrium state. It is due to the friction at the contact line. Indeed we have seen that higher is the coupling, higher is the friction coefficient so the velocity of the contact line will be smaller and the droplet will need more time to recover equilibrium.

Effect of the Weber number

We first look at the effect of the Weber number on the contact diameter. To vary this quantity, we will only change the impact velocity and keep constant the other parameters. In Figure 7 we show the maximum contact diameter for various Weber numbers. It shows that by increasing We, we increase the maximum contact diameter D_{max}. It is an expected result but we can already see that the wettability has an effect on this parameter. Indeed, points corresponding to different couplings do not collapse into a single curve. We will describe this effect in more details later on. By increasing the impact velocity we are thus able to tune the value of the maximum spreading within a considerable range (~ 140 nm) for a droplet of initial diameter of 34.6 nm.

We also recover another known result. For hydrophilic substrate, there is never rebound but for hydrophobic one, there can be one. Indeed, if we increase the Weber number, the droplet will splash at high We in the case of hydrophilic substrate but rebound in hydrophobic one.

This work is licensed under a Creative Commons 4.0 International License (CC BY-NC-ND 4.0).

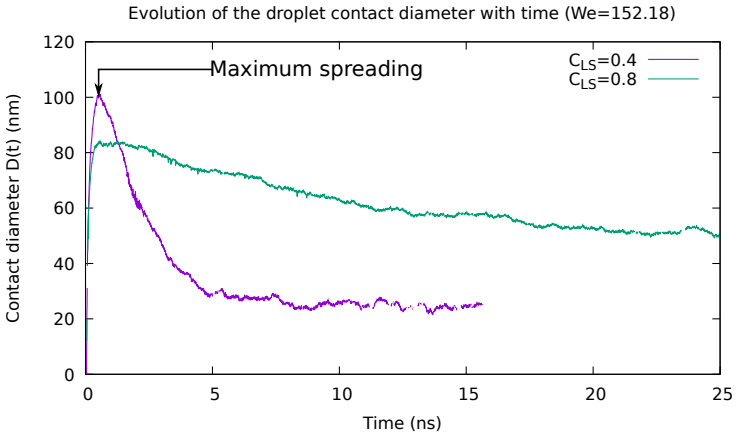

Figure 6. Spreading dynamics for a droplet impact – We is fixed and two wettabilities are considered

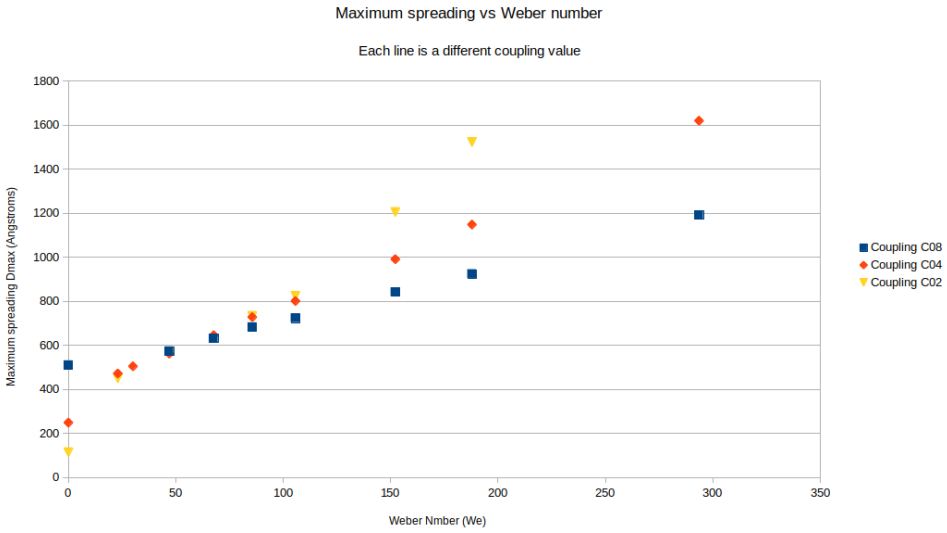

Figure 7. Maximum spreading for various Weber numbers

Effect of the wettability

In Figure 8 we show the dynamics of the contact diameter for various impact velocities and two different wettabilities. It is presented on a special scale so as to merge all the curves. This is a known results [16] and it thus shows that molecular dynamics is an appropriate tool to study this problem at the nano scale. The dotted black lines are the fitted curves to evaluate accuratly the value of the maximum contact diameter. Against, we use the polynomial ratio (7) to fit the data. These curves give a new result. Indeed if we compare the two graphs we see that the pic location and the pic width are different. The maximum spreading appends always faster if the couplings is smaller and the pic is also thinner. So the wettability affects two fundamental parameters of the impact dynamics. Indeed these observations are linked to the time at maximum spreading t_s (location of the pic) and the maximum spreading time $\Delta t_{\xi_{max}}$ (width of the pic). It means that even if the maximum spread factor is larger in the case of low coupling, the droplet will reach it in a shorter time period t_s. It can be understood in terms of friction effect. If the couplings is low, so the substrate hydrophobic, the friction will be small. The droplet will does dissipate less kinetic energy and reach the maximum spreading faster. It will also recede faster because the friction force acting against the receding will be smaller. These results shows the importance of molecular effects at this scale and the fact that known correlations must be revisited.

The other important effect of wettability has been introduced in the last section. Indeed the maximum spreading varies with the wettability and this variation depends on the Weber number. We thus introduce a modified Weber number which takes into account the wettability. We multiply the classic Weber number by a factor $1 - \cos\theta_{eq}$ so as to introduce the wettability. In Figure 9 we show the benefit of this modified Weber number for the maximum spreading study. It shows that if we introduce this wettability factor, all the points collapse into one virtual line. There must then be a general law which involves the equilibrium contact angle to predict the maximum spreading.

This work is licensed under a Creative Commons 4.0 International License (CC BY-NC-ND 4.0).

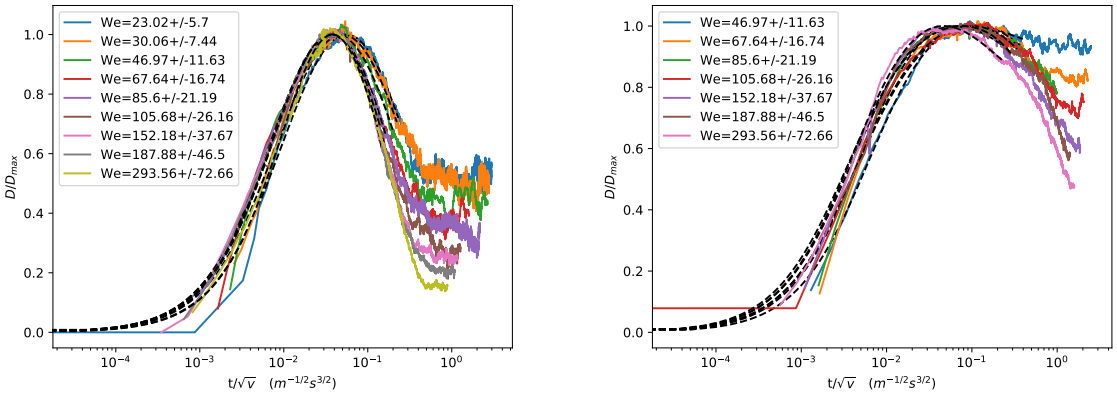

(a) C_{LS}=0.4 (b) C_{LS}=0.8

Figure 8. Contact diameter dynamics for various impact velocities

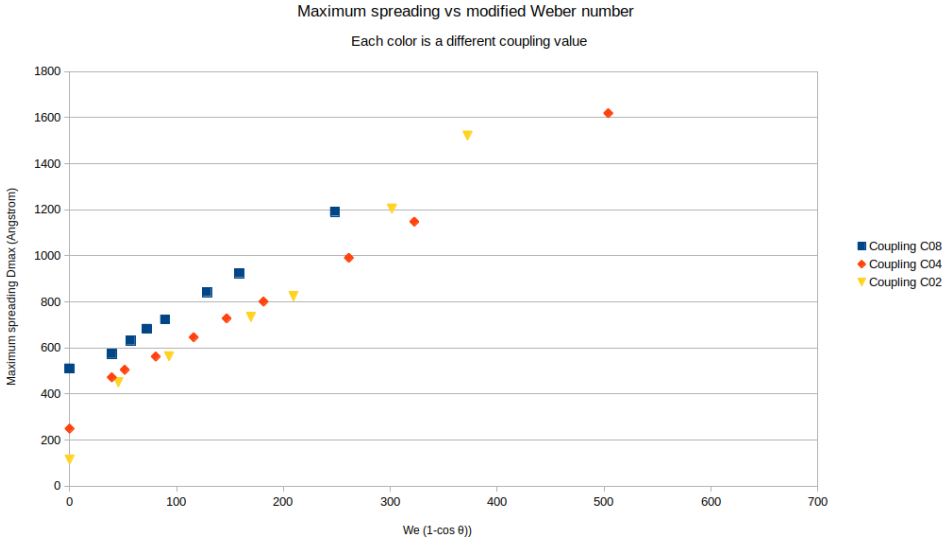

Figure 9. Maximum spreading for various modified Weber number

Conclusions

We have shown that in order to study droplet spreading dynamics, a quasi 2D slice model can be used. Indeed, we demonstrated that we are able to recover previous known results in terms of contact angles and frictions. This model allow us to consider the impacting drop problem because it enables to consider large system along x direction. We have also shown that molecular dynamics is a very good tool to understand the impact process at the nanoscale because it give access to molecular properties and flows.

We first recovered known results, the Weber number influences the maximum spreading. By increasing this number, we also increase the maximum contact diameter. We also recovered the transition between sticking drop and splashing drop or rebound in the case of hydrophobic substrate. Then we exposed the fact that the wettability has a crucial place in drop impact at the nano scale. Indeed, we showed that maximum spreading curves are collapsing only if we consider the wettability of the substrate with a specific factor. Finally we saw that the wettability also influence the time at maximum spreading and the spreading time, these values decrease with the wettability.

Acknowledgements

This research was partially funded by UMONS. Computational resources have been provided by the Consortium des Equipements de Calcul Intensif (CECI), funded by the Fonds de la Recherche Scientifique de Belgique (F.R.S.-FNRS) under Grant No. 2.5020.11

This work is licensed under a Creative Commons 4.0 International License (CC BY-NC-ND 4.0).

Nomenclature

V_{FENE}	finite extensible nonlinear elastic potential [J]
K_L	stiffness of molecular "springs" [$\mathrm{kg\ s^{-2}}$]
R_0	maximum extension length [m]
r	position [m]
K_S	stiffness of solid "springs" [$\mathrm{kg\ s^{-2}}$]
r_0	equilibrium position [m]
V_{ij}	pairwise Lennard-Jones potential [J]
C_{AB}	coupling between atoms of type "A" and type "B" [-]
σ_{ij}	effective molecular diameter [m]
r_{ij}	distance between atom i and atom j [m]
ε_{ij}	depth of the Lennard-Jones potential [J]
m	mass of an atom[kg]
v	velocity [$\mathrm{m\ s^{-1}}$]
k_B	Boltzmann constant [$\mathrm{J\ K^{-1}}$]
T	temperature [K]
$\mathcal{N}_\mathcal{A}$	Avogadro constant [$\mathrm{mol^{-1}}$]
ρ_L	liquid density [$\mathrm{kg\ m^{-3}}$]
ρ_0	density in the core of the droplet [$\mathrm{kg\ m^{-3}}$]
x_e	edge of the drop [m]
d	thickness of the liquid vacuum interface [m]
V_{CL}	velocity of the contact line [$\mathrm{m\ s^{-1}}$]
ζ_{CL}^0	friction coefficient at the contact line [$\mathrm{Pa\ s}$]
γ_L	surface tension of the liquid [$\mathrm{N\ m^{-1}}$]
θ_{eq}	equilibrium contact angle [-]
θ_D	dynamic contact angle [-]
R	Contact radius [m]
D	Contact diameter [m]
ξ	Spread factor [-]
D_0	Initial droplet diameter [m]
We	Weber number [-]
ξ_{max}	Maximum spread factor [-]
t_s	Spreading time [s]
$\Delta t_{\xi_{max}}$	Time at maximum spreading [s]

References

[1] Plimpton, S., 1995, *Journal of Computational Physics*, 117 (1), pp. 1-19.
[2] Fernandez-Toledano, J.-C., Blake, T.D., Lambert, P., De Coninck, J., 2017, *Advances in Colloid and Interface Science*, pp. 102-107.
[3] Fernandez-Toledano, J.-C., Blake, T.D., De Coninck, J., 2017, *Langmuir*, 33 (11), pp. 2929-2938.
[4] Fernandez-Toledano, J.-C., Blake, T.D., De Coninck, J., 2019, *Journal of Colloid and Interface Science*, 540, pp. 322-329.
[5] Bertrand, E., Blake, T.D., De Coninck, J., 2009, *Journal of Physics: Condensed Matter*, 21 (46), 464124.
[6] Blake, T.D., De Coninck, J., 2002, *Advances in Colloid and Interface Science*, 96, pp. 21-36.
[7] Scheller, B., Bousfield, D., 1995, *AIChE*, 41, pp. 1357-1367.
[8] Roisman, I.V., 2009, *Physics of Fluids*, 21, 052104.
[9] Clanet, C., Béguin, C., Richard, D., Quéré, D., 2004, *Journal of Fluid Mechanics*, 517, pp. 199-208.
[10] Mao, T., Kuhn, D., Tran, H., 1997, *AIChE*, 43, pp. 2169-2179.
[11] Pasandideh-Fard, M., Qiao, Y., Chandra, S., 1996, *Physics of Fluids*, 8, pp. 650-659.
[12] Kim, H.-Y., Chun., J.-H., 2001, *Physics of Fluids*, 13, pp. 643-659.
[13] Delplanque, J., Rangel, R., 1997, *Journal of Materials Science*, 32 (6), pp. 1519-1530.
[14] Attané, P., Girard, F., Morin, V., 2007, *Physics of Fluids*, 19, 012101.
[15] Stukowski, A., 2009, *Modelling and Simulation in Materials Science and Engineering*, 18 (1), 015012.
[16] Antonini, C., Amirfazli, A., Marengo, M., 2012, *Physics of Fluids*, 24 (134).

This work is licensed under a Creative Commons 4.0 International License (CC BY-NC-ND 4.0).